

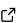
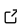
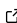
PeriDEM – High-fidelity modeling of granular media consisting of deformable complex-shaped particles

Prashant Kumar Jha ¹

¹ Department of Mechanical Engineering, South Dakota School of Mines and Technology, Rapid City, SD 57701, USA

DOI: [10.xxxxxx/draft](https://doi.org/10.xxxxxx/draft)

Software

- [Review](#) 
- [Repository](#) 
- [Archive](#) 

Editor: [Open Journals](#) 

Reviewers:

- [@openjournals](#)

Submitted: 01 January 1970

Published: unpublished

License

Authors of papers retain copyright and release the work under a Creative Commons Attribution 4.0 International License ([CC BY 4.0](#)).

Summary

Granular materials plays a crucial role in wide range of sectors including geotechnical, manufacturing, and mining. Predictive modeling of these materials under large loading becomes a challenging task due to deformation and breakage of particles and complex contact mechanism between complex-shaped particles undergoing considerable deformation. Focusing on the scenarios when particle deformation and breakage are crucial, PeriDEM model introduced in (Jha et al., 2021) is implemented in the PeriDEM library. The underlying idea is that individual particles are modeled as deformable solid using peridynamics theory, and the contact between two deforming particles are applied at locally at the contact region allowing modeling of complex-shaped particles. The integration of peridynamics within discrete element method (DEM) provides a flexible, hybrid framework that handles the contact mechanics at the particle boundary while accounting for the internal material response, including deformation and fracture. This opens up new avenues for exploring the interactions in granular systems, including developing constitutive laws for phenomenological continuum models, understanding effective behavior when subjected to large loading, and impact of particle shape on particle dynamics.

Statement of Need

Granular materials are prevalent in numerous industrial sectors, including geotechnical, manufacturing, and mining. Current modeling techniques such as DEM struggle with accurately capturing the behavior of granular materials under extreme conditions, especially when dealing with complex geometries and deformable particles. PeriDEM overcomes the challenges and implements a high-fidelity framework combining DEM and peridynamics to allow for accurate simulations of granular systems under extreme loading conditions. PeriDEM library makes the implementation of high-fidelity approach transparent. The library depends on very limited external libraries and is easier to build on ubuntu and mac systems allowing quick testing and extension to user specific needs.

Background

PeriDEM model was introduced in (Jha et al., 2021), where it demonstrated the ability to model both inter-particle contact and intra-particle fracture for arbitrarily shaped particles. The model is briefly described next.

35 Brief Introduction to PeriDEM Model

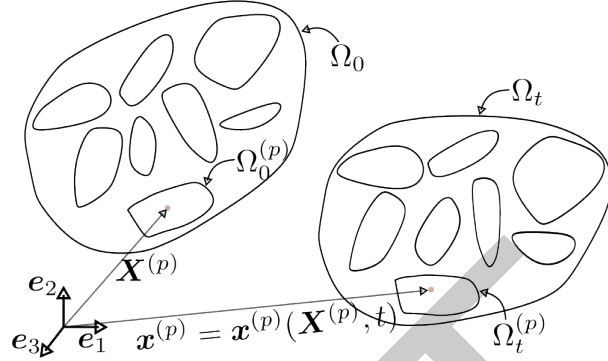


Figure 1: Motion of particle system.

36 Suppose a fixed frame of reference and $\{e_i\}_{i=1}^d$ are orthonormal bases. Consider a collection
 37 of N_P particles $\Omega_0^{(p)}$, $1 \leq p \leq N_P$, where $\Omega_0^{(p)} \subset \mathbb{R}^d$ with $d = 2, 3$ represents the initial
 38 configuration of particle p . Suppose $\Omega_0 \supset \cup_{p=1}^{N_P} \Omega_0^{(p)}$ is the domain containing all particles; see
 39 Figure 1. The particles in Ω_0 are dynamically evolving due to external boundary conditions and
 40 internal interactions; let $\Omega_t^{(p)}$ denote the configuration of particle p at time $t \in (0, t_F]$, and
 41 $\Omega_t \supset \cup_{p=1}^{N_P} \Omega_t^{(p)}$ domain containing all particles at that time. The motion $x^{(p)} = x^{(p)}(X^{(p)}, t)$
 42 takes point $X^{(p)} \in \Omega_0^{(p)}$ to $x^{(p)} \in \Omega_t^{(p)}$, and collectively, the motion is given by $x = x(X, t) \in$
 43 Ω_t for $X \in \Omega_0$. We assume the media is dry and not influenced by factors other than
 44 mechanical loading (e.g., moisture and temperature are not considered). The configuration of
 45 particles in Ω_t at time t depends on various factors, such as material and geometrical properties,
 46 contact mechanism, and external loading. Essentially, there are two types of interactions
 47 present in the media:

- 48 (1.) *Intra-particle interaction* that models the deformation and internal forces in the particle
 49 and
- 50 (2.) *Inter-particle interaction* that accounts for the contact between particles and the boundary
 51 of the domain the particles are contained in.

52 In DEM, the first interaction is ignored, assuming particle deformation is insignificant compared
 53 to the inter-particle interaction. On the other hand, PeriDEM, accounts for both interactions.

54 The balance of linear momentum for particle p , $1 \leq p \leq N_P$, takes the form:

$$\rho^{(p)} \ddot{u}^{(p)}(X, t) = f_{int}^{(p)}(X, t) + f_{ext}^{(p)}(X, t), \quad \forall (X, t) \in \Omega_0^{(p)} \times (0, t_F), \quad (1)$$

55 where $\rho^{(p)}$, $f_{int}^{(p)}$, and $f_{ext}^{(p)}$ are density, and internal and external force densities. The above equa-
 56 tion is complemented with initial conditions, $u^{(p)}(X, 0) = u_0^{(p)}(X)$, $\dot{u}^{(p)}(X, 0) = \dot{u}_0^{(p)}(X)$, $X \in$
 57 $\Omega_0^{(p)}$.

58 Internal force - State-based peridynamics

59 Since all expressions in this paragraph are for a fixed particle p , we drop the superscript p ,
 60 noting that material properties and other quantities can depend on the particle p . Following
 61 (Silling et al., 2007) and simplified expression of state-based peridynamics force in (Jha et al.,
 62 2021), the internal force takes the form, for $X \in \Omega_0^{(p)}$,

$$f_{int}^{(p)}(X, t) = \int_{B_\epsilon(X) \cap \Omega_0^{(p)}} (T_X(Y) - T_Y(X)) \, dY, \quad (2)$$

where $T_X(Y) - T_Y(X)$ is the force on X due to nonlocal interaction with Y . Let $R = |Y - X|$ be the reference bond length, $r = |x(Y) - x(X)|$ current bond length, $s(Y, X) = (r - R)/R$ bond strain, then $T_X(Y)$ is given by (Jha et al., 2021; Silling et al., 2007)

$$T_X(Y) = h(s)J(R/\epsilon) \left[R\theta_X \left(\frac{3\kappa}{m_X} - \frac{15G}{3m_X} \right) + (r - R)\frac{15G}{m_X} \right] \frac{x(Y) - x(X)}{|x(Y) - x(X)|}, \quad (3)$$

where

$$\begin{aligned} m_X &= \int_{B_\epsilon(X) \cap \Omega_0^{(p)}} R^2 J(R/\epsilon) dY, \\ \theta_X &= h(s) \frac{3}{m_X} \int_{B_\epsilon(X) \cap \Omega_0^{(p)}} (r - R) R J(R/\epsilon) dY, \\ h(s) &= \begin{cases} 1, & \text{if } s < s_0 := \sqrt{\frac{\mathcal{G}_c}{(3G + (3/4)^4[\kappa - 5G/3])\epsilon}}, \\ 0, & \text{otherwise.} \end{cases} \end{aligned} \quad (4)$$

In the above, $J : [0, \infty) \rightarrow \mathbb{R}$ is the influence function, κ, G, \mathcal{G}_c are bulk and shear moduli and critical energy release rate, respectively. These parameters, including nonlocal length scale ϵ , could depend on the particle p .

DEM-inspired contact forces

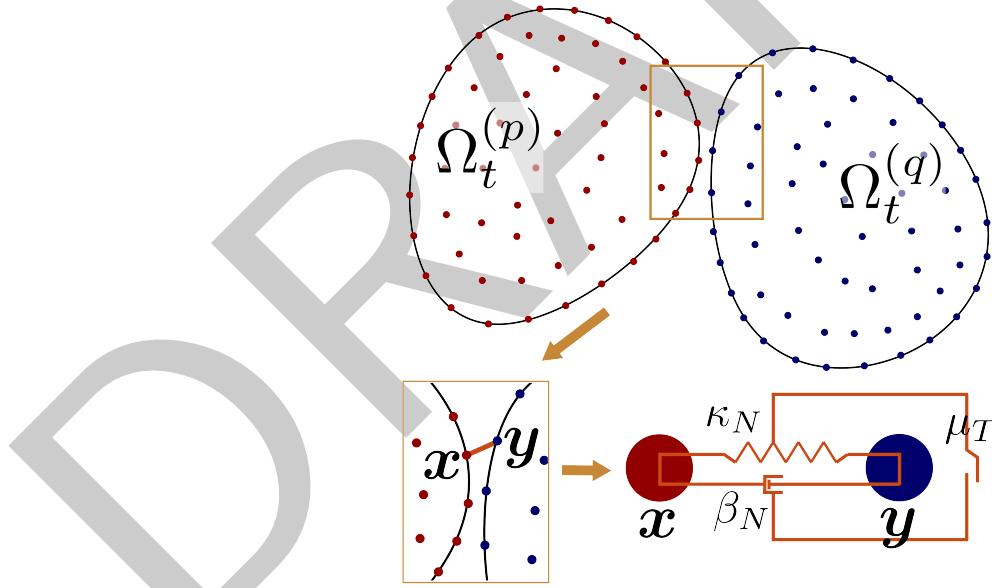


Figure 2: High-resolution contact approach in PeriDEM model for granular materials between arbitrarily-shaped particles.

The external force density $f_{ext}^{(p)}$ is generally expressed as

$$f_{ext}^{(p)} = \rho^{(p)}b + f^{\Omega_0, (p)} + \sum_{q \neq p} f^{(q), (p)}, \quad (5)$$

where b is body force per unit mass, $f^{\Omega_0, (p)}$ and $f^{(q), (p)}$ are contact forces due to interaction between particle p and container Ω_0 and neighboring particles q , respectively. In (Jha et al., 2021), the contact between two particles is applied locally where the contact takes place; this is exemplified in Figure 2 where contact between points y and x of two distinct particles p

and q is activated when they get sufficiently close. The contact forces are shown using a spring-dashpot-slider system. To fix the contact forces, consider a point $X \in \Omega_0^{(p)}$ and let $R_c^{(q),(p)}$ be the critical contact radius (points in particles p and q interact if the distance is below this critical distance). Further, define the relative distance between two points $Y \in \Omega_0^{(q)}$ and $X \in \Omega^{(p)}$ and normal and tangential directions as follows:

$$\begin{aligned}\Delta^{(q),(p)}(Y, X) &= |x^{(q)}(Y) - x^{(p)}(X)| - R_c^{(q),(p)}, \\ e_N^{(q),(p)}(Y, X) &= \frac{x^{(q)}(Y) - x^{(p)}(X)}{|x^{(q)}(Y) - x^{(p)}(X)|}, \\ e_T^{(q),(p)}(Y, X) &= [I - e_N^{(q),(p)}(Y, X) \otimes e_N^{(q),(p)}(Y, X)] \frac{\dot{x}^{(q)}(Y) - \dot{x}^{(p)}(X)}{|\dot{x}^{(q)}(Y) - \dot{x}^{(p)}(X)|}.\end{aligned}\quad (6)$$

Then the force on particle p due to contact with particle q can be written as (Jha et al., 2021):

$$f^{(q),(p)}(X, t) = \int_{Y \in \Omega_0^{(q)} \cap B_{R_c^{(q),(p)}}(X)} (f_N^{(q),(p)}(Y, X) + f_T^{(q),(p)}(Y, X)) dY, \quad (7)$$

with normal and tangential forces following (Desai et al., 2019; Jha et al., 2021) given by, if $\Delta^{(q),(p)}(Y, X) < 0$,

$$f_N^{(q),(p)}(Y, X) = [\kappa_N^{(q),(p)} \Delta^{(q),(p)}(Y, X) - \beta_N^{(q),(p)} \dot{\Delta}^{(q),(p)}(Y, X)], \quad (8)$$

else $f_N^{(q),(p)}(Y, X) = 0$, and

$$f_T^{(q),(p)}(Y, X) = -\mu_T^{(q),(p)} |f_N^{(q),(p)}(Y, X)| e_T^{(q),(p)}. \quad (9)$$

Implementation

PeriDEM is implemented as an open-source library in GitHub; see PeriDEM. It is based on C++, and uses only handful external libraries which are included in the library in the external folder, allowing the code to be built and tested in ubuntu and mac systems relatively easily. Taskflow (Huang et al., 2021) is used for asynchronous multithreaded computation and Nanoflann (Blanco & Rai, 2014) for tree search to calculate neighbors for contact forces. MPI and metis (Karypis & Kumar, 1997) have recently been integrated to implement the distributed parallelism in near future. VTK is used to output the simulation files which can be visualized using paraview.

Features

- Hybrid modeling using peridynamics and DEM for intra-particle and inter-particle interactions.
- Support for complex shaped particles, allowing for realistic simulation scenarios.
- MPI will be used for distributed computing in near future.
- Future work includes developing an adaptive modeling approach to enhance efficiency without compromising accuracy.

Brief implementation details

The main implementation of the model is carried out in the model directory [dem](#). The model is implemented in class [DEMModel](#). Function `DEMModel::run()` performs the simulation. We next look at some key methods in `DEMModel` in more details:

105 **DEMModel::run()**

106 This function does three tasks:

```
void model::DEMModel::run(inp::Input *deck) {
    // initialize data
    init();

    // check for restart
    if (d_modelDeck_p->d_isRestartActive)
        restart(deck);

    // integrate in time
    integrate();
}
```

107 In `DEMModel::init()`, the simulation is prepared by reading the input files (such as `.yaml`,
108 `.msh`, `particle_locations.csv` files).

109 **DEMModel::integrate()**

110 Key steps in `DEMModel::integrate()` are

```
void model::DEMModel::run(inp::Input *deck) {
    // apply initial condition
    if (d_n == 0)
        applyInitialCondition();

    // apply loading
    computeExternalDisplacementBC();
    computeForces();

    // time step
    for (size_t i = d_n; i < d_modelDeck_p->d_Nt; i++) {
        // advance simulation to next step
        integrateStep();

        // perform output if needed
        output();
    }
}
```

111 In `DEMModel::integrateStep()`, we either utilize the central-difference scheme, imple-
112 mented in `DEMModel::integrateCD()`, or the velocity-verlet scheme, implemented in
113 `DEMModel::integrateVerlet()`. As an example, we look at `DEMModel::integrateCD()`
114 method below:

```
void model::DEMModel::integrateVerlet() {
    // update current position, displacement, and velocity of nodes
    {
        tf::Executor executor(util::parallel::getNThreads());
        tf::Taskflow taskflow;

        taskflow.for_each_index(
            (std::size_t) 0, d_fPdCompNodes.size(), (std::size_t) 1,
            [this, dt, dim](std::size_t II) {
                auto i = this->d_fPdCompNodes[II];
```

```

const auto rho = this->getDensity(i);
const auto &fix = this->d_fix[i];

for (int dof = 0; dof < dim; dof++) {
    if (util::methods::isFree(fix, dof)) {
        this->d_v[i][dof] += 0.5 * (dt / rho) * this->d_f[i][dof];
        this->d_u[i][dof] += dt * this->d_v[i][dof];
        this->d_x[i][dof] += dt * this->d_v[i][dof];
    }
}
} // loop over nodes
); // for_each

executor.run(taskflow).get();
}

// advance time
d_n++;
d_time += dt;

// update displacement bc
computeExternalDisplacementBC();

// compute force
computeForces();

// update velocity of nodes (similar to the above)
}

```

115 **DEMModel::computeForces()**

116 The key method in time integration is `DEMModel::computeForces()` In this function, we
 117 compute internal and external forces at each node of a particle and also account for the
 118 external boundary conditions. This function looks like

```

void model::DEMModel::computeForces() {
    // update the point cloud (make sure that d_x is updated along with displacement)
    auto pt_cloud_update_time = d_nsearch_p->updatePointCloud(d_x, true);
    pt_cloud_update_time += d_nsearch_p->setInputCloud();

    // reset forces to zero ...

    // compute peridynamic forces
    computePeridynamicForces();

    // compute contact forces between particles
    computeContactForces();

    // Compute external forces
    computeExternalForces();
}

```

119 **Further reading**

120 Above gives the basic idea of simulation steps. For more thorough understanding of the
 121 implementation, interested readers can look at [demModel.cpp](#).

122 Examples

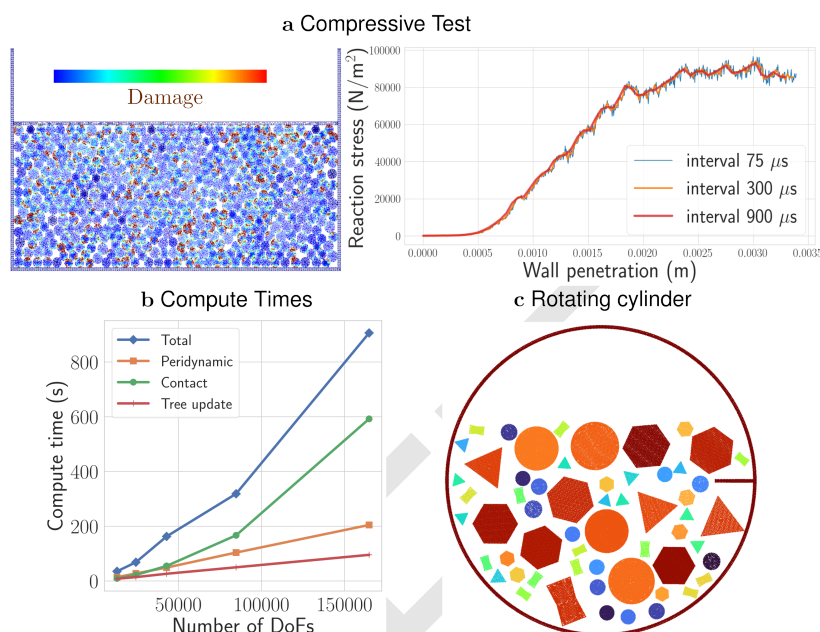


Figure 3: (a) Nonlinear response under compression, (b) exponential growth of compute time due to nonlocality of internal and contact forces, and (c) rotating cylinder with nonspherical particles.

123 Examples are described in [examples/README.md](#) of the library. One of the key result is
 124 the compression of 502 circular and hexagon particles in a rectangular container by moving
 125 the top wall. The stress on the moving wall as a function of wall penetration becomes
 126 increasingly nonlinear, and media shows signs of yielding as the damage becomes extensive; see
 127 [Figure 3a](#). Preliminary compute time analysis with an increasing number of particles shows an
 128 exponential increase in compute time of contact and peridynamics forces, which is unsurprising
 129 as both computations are nonlocal. Demonstration examples also include attrition of various
 130 non-circular particles in a rotating cylinder [Figure 3c](#).

131 References

- 132 Blanco, J. L., & Rai, P. K. (2014). *Nanoflann: A C++ header-only fork of FLANN, a library*
 133 *for nearest neighbor (NN) with KD-trees*. <https://github.com/jlblancoc/nanoflann>.
- 134 Desai, P. S., Mehta, A., Dougherty, P. S., & Higgs III, C. F. (2019). A rheometry based
 135 calibration of a first-order DEM model to generate virtual avatars of metal additive
 136 manufacturing (AM) powders. *Powder Technology*, 342, 441–456.
- 137 Huang, T.-W., Lin, D.-L., Lin, C.-X., & Lin, Y. (2021). Taskflow: A lightweight parallel and
 138 heterogeneous task graph computing system. *IEEE Transactions on Parallel and Distributed*
 139 *Systems*, 33(6), 1303–1320.
- 140 Jha, P. K., Desai, P. S., Bhattacharya, D., & Lipton, R. (2021). Peridynamics-based discrete
 141 element method (PeriDEM) model of granular systems involving breakage of arbitrarily
 142 shaped particles. *Journal of the Mechanics and Physics of Solids*, 151, 104376.
- 143 Karypis, G., & Kumar, V. (1997). *METIS: A software package for partitioning unstructured*
 144 *graphs, partitioning meshes, and computing fill-reducing orderings of sparse matrices*.
- 145 Silling, S. A., Epton, M., Weckner, O., Xu, J., & Askari, E. (2007). Peridynamic states and

DRAFT